A Squeezed Modulation Signal Bispectrum Method for Motor Current Signals Based Gear Fault Diagnosis

Yuandong Xu, Xiaoli Tang, *Member, IEEE*, Xiuquan Sun, Fengshou Gu and Andrew D. Ball

***Abstract*— Electromechanical systems as the prime power source are widely employed in industry. To ensure the high productivity and safety of the motor-gear system, motor current signature analysis (MCSA) becomes a cost-effective and effective approach to health condition monitoring of motors and gears simultaneously. Generally, working conditions of the motor-gear system can be separated into stationary and nonstationary working conditions. The nonstationary working conditions usually refer to varying speeds, which have been broadly investigated in the angular domain analysis and time-frequency analysis. The stationary working conditions are assumed to have a constant rotating speed which is an ideal scenario but practically the rotating speed varies slightly with randomness. The random speed variation seems neglectable but it actually spreads the energy into adjacent frequency bins, which thus attenuates the amplitude of fault signatures and leads to inaccurate fault diagnosis. To address this issue, a Squeezed Modulation Signal Bispectrum (MSB) approach is developed to concentrate the leaked energy for accurately diagnosing gear faults with motor current signals. The Squeezed MSB concentrates the energy in the frequency domain along the time axis to overcome the random speed oscillation induced energy leakage and then, demodulates and aligns the modulation fault signatures from the squeezed spectra for ensemble averaging to further enhance fault signatures. The simulation study shows the performance of the proposed method under different levels of random speed variation and the experimental studies demonstrate the effectiveness of the Squeezed MSB for diagnosing gear tooth breakage faults under a wide range of working conditions.**

***Index Terms*— Random speed variation, Squeezed MSB, fault diagnosis, gears, motor current signature analysis**

I. INTRODUCTION

MACHINE condition monitoring (CM) can avoid potential failure and prevent catastrophic accidents of rotating machines. Effective fault detection and diagnosis techniques attract large quantities of research interest due to their significant benefits in maintenance schemes [1]. Electromechanical systems are widely used in industry and typically contain induction motors for powering sources and gearboxes for speed and load regulators. However, motors and gears are prone to various faults, and these malfunctions can lead to low productivity and even catastrophic accidents. Motor current signature analysis (MCSA) has been investigated for over 20 years to achieve effective condition monitoring of electromechanical systems [2]. Motor current signals can be obtained from a cost-effective and non-intrusive transducer that be easily clamped on the power cables. With the wide use of electromechanical systems, MCSA attracts more and more researchers to extensively study, improve and deploy effective and efficient fault detection and diagnostics of electromechanical systems [3].

Motor current signals contain valuable information on the health conditions of electromechanical systems. Although the motor current signal is widely explored for the diagnosis of various motor faults, a few studies have been carried out on MCSA based gear fault detection and diagnosis. Kar and Mohanty [4] firstly employed MSCA to monitor gear defects and they indicated that MCSA is an alternative to the conventional vibration based condition monitoring. The application of MCSA in fault diagnosis of the planetary gearbox is adopted more and more owing to that the motor current is free of transmission paths and sensitive to torque oscillation. Zhang *et al*. [5] investigated the residual signals around the resonance frequency after removing the multiple harmonics in the angular domain and the higher amplitude shows the proposed method is sensitive to planetary gearbox faults. Gao *et al.* [6] explained the generated amplitude modulation and frequency modulation in motor current signals when the fault occurs on the planet and sun gears. These studies show promising diagnostic results even through simple FFT-based spectrum analysis.

To extract more accurate monitoring information from the noisy motor current signal, Gu *et al*. [7] developed the Modulation Signal Bispectrum (MSB) approach using the phase alignment characteristic to suppress strong background noise in motor current signals for fault diagnosis of reciprocating compressors. With more investigation, Gu *et al*.

(*Corresponding author: Xiaoli Tang*)

Yuandong Xu is with Dynamics Group, Department of Mechanical Engineering, Imperial College London, London SW7 2AZ, UK (e-mail: y.xu@imperial.ac.uk).

Xiaoli Tang is with School of Engineering and Technology, Aston University, Birmingham B4 7ET, UK (e-mail: x.tang4@ aston.ac.uk).

Xiuquan Sun, Fengshou Gu and Andrew D. Ball are with Centre for Efficiency and Performance Engineering, University of Huddersfield, Huddersfield HD1 3DH, UK (e-mail: x.sun2@hud.ac.uk; F.Gu@hud.ac.uk; A.Ball@hud.ac.uk).

[8] applied the MSB analysis to induction motor stator currents for diagnosing broken rotor bar faults. The MSB approach is also employed to monitor gear wear by Zhang *et al*. [9] using motor current signals. However, as the MSB method is developed based on the conventional Fourier transform, its performance can be degraded by the problem of spectral leakage and limited capabilities when applying Fourier transform to nonstationary motor current signals. In particular, when a localized fault occurs on meshing gears such as a broken tooth, sudden changes in mesh stiffness results in additional torque oscillation relating to rotating frequency. The speed variation results in amplitude and frequency modulation at the same time [10]. Both amplitude modulation and frequency modulation are based on the hypothesis of constant working conditions which assumes the periodic variation is identical in each revolution and the average rotating speeds of every revolution are exactly the same. However, stationary signals are always ideal, and nonstationary signals are by nature. It is observed that the random speed variation exists in the so-called constant working conditions during the experiments. Fig. 1 gives an example of the speed oscillation at stable working conditions from a motor-gear rig shown in Fig. 7, and an engine test rig, respectively. The probability density functions (PDFs) are calculated by the normalized rotating speeds of each revolution at stable working conditions. Although the test rigs were well controlled by the advanced control system in the laboratory, the speed variation between each revolution is still obvious. The PDFs of rotating speeds from both test rigs obey the Gaussian distribution.

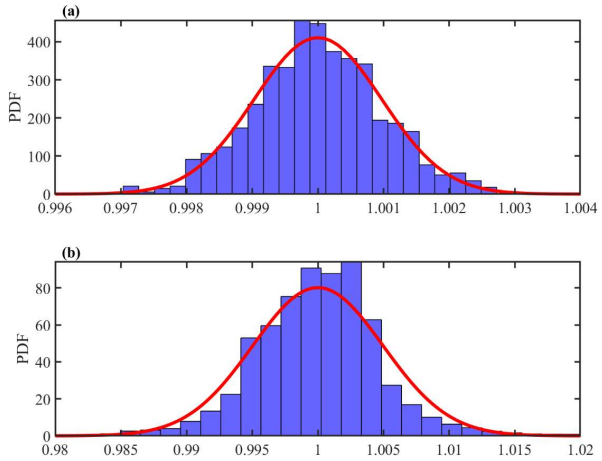

Fig. 1. Example of speed variation: (a) motor-gear tests; (b) engine tests.

Literally, spectral leakage happens in the discrete Fourier transform due to the non-integer number of periods of a periodic signal [11]. The leakage concept is extended to this specific phenomenon because of the quick random oscillation of the signal components. The random speed variation leads to the energy blurred spectrum and makes Fourier transform based approaches inaccurate. This problem is different from the frequently discussed nonstationary working conditions which attract large quantities of researchers to study vibroacoustic signals under relatively slow speed variation [12], especially owing to the exponentially growing number of wind turbines. The mentioned random speed variation is a relatively fast oscillation which has not been addressed in the literature. It is worth addressing again that the random speed variation between revolutions around the average speed here is not the well-known modulation phenomenon in the instantaneous angular speed (IAS) or vibrations. The main difference between random speed variation and IAS modulation is that the random speed variation does not show any deterministic characteristics. The random speed variation in this paper mainly comes from the uncertainty of power sources and external loads under the nominal constant working conditions. The random speed variation seems to be within another popular topic of cyclostationary analysis. The definition of a cyclostationary signal is that it exhibits some hidden periodicity of its energy flow [13]. The random speed variation alters the instantaneous frequency of a periodic signal, leading to the random variation of the signal energy. Therefore, cyclostationary analysis cannot accurately describe the random speed variation, which is demonstrated in this simulation study. To the best of the authors' knowledge, random speed variation has not been thoroughly discussed for fault detection and diagnosis of rotating machines. There is no doubt that the famous time synchronous averaging (TSA) method [14] can suppress the random speed variation but it requires accurate tacho signals which are not always available and accessible for rotating machines in harsh working environments.

One contribution of this study is to spotlight the random speed variation of rotating machines under constant working conditions. This nonstationarity aggravates the spectral leakage in the frequency domain and weakens the gear fault signatures in motor current signals. In this paper, the gear fault induced sidebands around the supply frequency with random speed variation is analytically characterized to show the modulation with nonstationary sidebands. Another main contribution is to develop a Squeezed MSB approach to concentrate the leaked energy to demodulate the reliable gear signatures from motor current signals. The proposed method extends the capability of the conventional MSB method and significantly improves the diagnostic accuracy under random speed variations. The remaining contents of this paper are organized as follows. The theoretical characteristics of motor current signals under tooth breakage faults and the algorithm of the Squeezed MSB method are given in Section II. The simulation and experimental studies are introduced and discussed in Section III and Section IV, respectively. Finally, conclusions are drawn in Section V.

II. Theoretical Background

A. Theoretical Characteristics of Motor Current Signals under Tooth Breakage Faults

The ideal electromagnetic relationship of induction motors can be represented by one of the three phases. In this paper, phase A current is used to discuss the effect of random speed oscillation. For a healthy induction motor, its current signal of phase A can be expressed as

$$i_A = \sqrt{2} I \cos(2\pi f_s t - \alpha_I) \quad (1)$$

where, I is the root mean square (RMS) of the supply current;

f_s is the fundamental frequency of electrical supply; α_I is the phase of the current referring to supply voltage. Correspondingly, the magnetic flux in the motor stator is

$$\phi_A = \sqrt{2}\phi\, cos\left(2\pi f_s t - \alpha_\phi\right) \tag{2}$$

where, ϕ is the RMS of the flux linkage and α_ϕ is the phase of flux. The electrical torque produced by the interaction of current and flux can be expressed as

$$T = 3P\phi I\, sin\left(\alpha_I - \alpha_\phi\right) \tag{3}$$

in which, P is the number of pole pairs.

The localized fault on gears leads to abnormal torque fluctuation and the electric torque interaction with the fundamental flux can be calculated by

$$T_e = \Im\left(P\vec{\phi}\,\vec{I}_F^{*}\right) \tag{4}$$

where, $\Im(\ )$ is the imaginary part of a complex number. Considering $\Delta f_F(t)$ is the random time-varying frequency around the average rotating frequency $\bar{f}_F$ of the faulty gear, the torque oscillation yields

$$\Delta T(t) = 3P\phi I_F \sin\left(\int 2\pi\left(\bar{f}_F + \Delta f_F(t)\right)dt - \alpha_\phi + \alpha_F\right) \tag{5}$$

which causes the oscillation of angular displacement.

$$\begin{aligned}\Delta\theta(t) &= \iint \frac{P}{J}\Delta T(t)dt \\ &= \frac{3P^2\phi I_F}{J}\iint \sin\left(\int 2\pi\left(\bar{f}_F + \Delta f_F(t)\right)dt - \alpha_\phi + \alpha_F\right)dt\end{aligned} \tag{6}$$

where, J is the inertia of the rotor system of the motor. In general, the random speed oscillation $\Delta f_F(t)$ is much smaller than the average speed $\bar{f}_F$. The $\Delta f_F(t)$ induced amplitude variation is omitted in the integral process and the angular displacement can be expressed as

$$\Delta\theta(t) = -\frac{3P^2\phi I_F}{4\pi^2\bar{f}_F^{\,2}J}\sin\left(\int 2\pi\left(\bar{f}_F + \Delta f_F(t)\right)dt - \alpha_\phi + \alpha_F\right) \tag{7}$$

Due to the oscillation of the angular displacement, the flux linkage phase in (2) becomes

$$\begin{aligned}\phi_A^F &= \sqrt{2}\phi\cos\left(2\pi f_s t - \alpha_\phi + \Delta\theta(t)\right) \\ &\approx \sqrt{2}\phi\left[\cos\left(2\pi f_s t - \alpha_\phi\right) - \sin\left(2\pi f_s t - \alpha_\phi\right)\Delta\theta(t)\right] \\ &= \sqrt{2}\phi\cos\left(2\pi f_s t - \alpha_\phi\right) \\ &+\Delta\phi_F\cos\left(\int 2\pi\left(f_s + \bar{f}_F + \Delta f_F(t)\right)dt - 2\alpha_\phi + \alpha_F\right) \\ &-\Delta\phi_F\cos\left(\int 2\pi\left(f_s - \bar{f}_F - \Delta f_F(t)\right)dt - \alpha_F\right)\end{aligned} \tag{8}$$

where, $\Delta\phi_F = 3\sqrt{2}P^2\phi^2 I_F/\left(8\pi^2\bar{f}_F^{\,2}J\right)$. The derivative of the flux linkage is the electromotive force (EMF), yielding

$$\begin{aligned}E_A^F &= -2\sqrt{2}\pi\phi f_s\sin\left(2\pi f_s t - \alpha_\phi\right) \\ &-2\pi\Delta\phi_F\left(f_s + \bar{f}_F + \Delta f_F(t)\right) \\ &\sin\left(\int 2\pi\left(f_s + \bar{f}_F + \Delta f_F(t)\right)dt - 2\alpha_\phi + \alpha_F\right) \\ &+2\pi\Delta\phi_F\left(f_s - \bar{f}_F - \Delta f_F(t)\right) \\ &\sin\left(\int 2\pi\left(f_s - \bar{f}_F - \Delta f_F(t)\right)dt - \alpha_F\right)\end{aligned} \tag{9}$$

The derivative of the flux linkage is the EMFs. The first term in (9) generates the fundamental EMF and the other two terms lead to lower and upper sidebands around the fundamental EMF. The amplitude of the impedance increases with frequency and the phase of the impedance decreases with frequency. The equivalent winding impedance at the supply frequency is Ze^{α_ϕ} and the impedances of two sideband components are $(Z - \Delta Z_l)e^{\varphi_Z + \varphi_{\Delta Z_l}}$ and $(Z + \Delta Z_u)e^{\varphi_Z - \varphi_{\Delta Z_u}}$. Consequently, the motor current signal can be expressed as

$$\begin{aligned}i_A^F &= -\frac{2\sqrt{2}\pi\phi f_s}{Z}\sin\left(2\pi f_s t - \alpha_\phi - \alpha_Z\right) \\ &-\frac{2\pi\Delta\phi_F\left(f_s + \bar{f}_F + \Delta f_F(t)\right)}{Z + \Delta Z_u} \\ &\sin\left(\int 2\pi\left(f_s + \bar{f}_F + \Delta f_F(t)\right)dt - 2\alpha_\phi + \alpha_F - \varphi_Z + \varphi_{\Delta Z_u}\right) \\ &+\frac{2\pi\Delta\phi_F\left(f_s - \bar{f}_F - \Delta f_F(t)\right)}{Z - \Delta Z_l} \\ &\sin\left(\int 2\pi\left(f_s - \bar{f}_F - \Delta f_F(t)\right)dt - \alpha_F - \varphi_Z - \varphi_{\Delta Z_l}\right)\end{aligned} \tag{10}$$

The localized gear fault results in additional sidebands of the shaft rotating frequency around the supply frequency of the motor current signals. The appropriate combination of phases between two sidebands and carrier components can eliminate the variation, leading to the reputational MSB approach. However, the MSB approach is most effective when dealing with stationary signals [15], [16]. The random speed variation $\Delta f_F(t)$ leads to the dissipation of energy into the adjacent frequency bins, which aggravates the performance of the MSB method and makes the fault detection and diagnosis not reliable in various working conditions. To enhance the capability of the MSB approach, a Squeezed MSB method is developed to handle the influence of the locally varying rotating speeds.

B. Algorithm of the Squeezed Modulation Signal Bispectrum

For a given signal $x(t) \in L^1(R)$, its short-time Fourier transform (STFT) is

$$\begin{aligned}S(\eta, t) &= \int_{-\infty}^{+\infty} x(\xi)g^*(\xi - t)e^{-i2\pi\eta t}\,d\xi \\ &= \int_{-\infty}^{+\infty} x(\xi)g(\xi - t)e^{-i2\pi\eta t}\,d\xi \\ &= M(\eta, t)e^{i\phi(\eta,t)}\end{aligned} \tag{11}$$

where $g(t)$ is a shifting window function and $g^*(t)$ is its complex conjugate. $M(\eta, t)$ and $\phi(\eta, t)$ are the magnitudes and phase of $S(\eta, t)$, respectively. To enhance the stationary modulation fault signatures, the MSB developed by Gu *et al.* [8] is defined as

$$B_{MS}(f_x, f_c) = \frac{1}{T}\int_0^T S(f_c + f_x, t)S(f_c - f_x, t)S^*(f_c, t)S^*(f_c, t)dt \tag{12}$$

where, f_c and f_x denote the frequencies of the carrier and modulated signals, respectively. The integral represents the averaging procedure of MSB for noise reduction owing to the phase alignment of modulation signals in MSB.

However, due to the varying speeds and spectral leakage, the spectrum is usually energy-blurred, even with the application of windows. To overcome this issue, a series of time-frequency analysis approaches are developed to concentrate the leaked energy into the main lobe. It can be seen from (11) that the local instantaneous frequency can be estimated as

$$\begin{aligned}\widehat{\omega}(\eta, t) &= \partial_t\phi(\eta, t) \\ &= \Re\left\{\frac{1}{i2\pi}\frac{\partial_t S(\eta, t)}{S(\eta, t)}\right\}\end{aligned} \tag{13}$$

This operator estimates the instantaneous frequency of the signal at time t and frequency η.

With this estimator, the coefficients $S(\eta, t)$ can be moved

from (η, t) to $(\hat{\omega}(\eta, t), t)$ which forms a more concentrated time-frequency representation. This approach is named the synchrosqueezing transform (SST) [17], which yields

$$S_S(f,t) = \frac{1}{g^*(0)} \int S(\eta, t)\delta(f - \hat{\omega}(\eta, t))d\eta \quad (14)$$

The synchrosqueezing transform is an effective method in time-frequency analysis [18], [19]. Owing to the property of energy concentration, the synchrosqueezing transform can improve the random speed variation induced energy-blurred spectrum. Therefore, the frequency assignment operator in the synchrosqueezing transform can be embedded into the conventional MSB method to tackle the random speed variation induced nonstationary signals. The Squeezed MSB firstly concentrates the energy in the frequency domain along the time axis to improve the random speed oscillation induced energy blur and then the three-dimensional MSB matrix is calculated in respect of each frequency slice in the time-frequency representation, yielding

$$B_{TMS}(f_x, f_c, t) = S_S(f_c + f_x, t)S_S(f_c - f_x, t)S_S^*(f_c, t)S_S^*(f_c, t) \quad (15)$$

Due to the random speed oscillation, the instantaneous modulation frequency f_x is not constant in the MSB matrix. The direct averaging along the time axis spreads the energy again into the adjacent frequency bins, which reduces the sparsity of the bispectrum and underestimates the strength of the modulation component. Therefore, the reassignment of the modulation frequency f_x is necessary to increase the accuracy of the demodulation analysis. To extract the ridge of the modulation frequency in the MSB matrix $B_{TMS}(f_x, f_c, t)$, the classic forward/backward approach for different initializations in [20] is used in this paper. As the modulation frequency of the gear fault is the shaft rotating frequency, the frequency band of the ridge extraction can be limited to several hertz because only one ridge is required to be extracted as the modulation frequency. Based on the extracted ridge of the modulation frequency, the reassignment process of the MSB matrix can be expressed as

$$\hat{B}_{TMS}(f_x, f_c, t) = B_{TMS}(f_x, f_c, t) * \delta\left(\overline{\omega_{f_x}}(f_x, f_c, t)\right), \quad \forall\{f_x \in \mathbb{R}, |\Delta f_x| \le \Delta_f\} \quad (16)$$

with

$$\Delta f_x = \omega(f_x, f_c, t) - \overline{\omega_{f_x}}(f_x, f_c, t) \quad (17)$$

where, $\omega(f_x, f_c, t)$ is the instantaneous bifrequency of the MSB matrix. $\overline{\omega_{f_x}}(f_x, f_c, t)$ is the average of the modulation frequency f_x in the bifrequency planes for the carrier frequency f_c. $\delta(\ )$ is the Dirac delta function. Δ_f is the threshold that selects the limited variation of the estimated instantaneous frequency. The ensemble averaging operation is then conducted to enhance the modulation signatures, which can be expressed as

$$B_{SMS}(f_x, f_c) = \frac{1}{T}\int_0^T \hat{B}_{TMS}(f_x, f_c, t)dt \quad (18)$$

Coherence is a measure of the identity of the $\hat{B}_{TMS}(f_x, f_c, t)$ magnitudes along the time axis t, yielding

$$CB_{SMS}(f_x, f_c) = \frac{\int_0^T \hat{B}_{TMS}(f_x, f_c, t)dt}{\int_0^T |\hat{B}_{TMS}(f_x, f_c, t)|dt} \quad (19)$$

The developed Squeezed MSB method can suppress the random speed oscillation induced energy blur phenomenon and concentrate the leaked energy back to the main frequency component. With concentrated energy to the main lobe, the extracted fault signatures can reflect the fault severity more accurately.

III. Simulation Study

To demonstrate the performance of the developed Squeezed MSB approach, a simulated current signal according to (10) is created to represent the modulation phenomenon and the random variation of rotating speeds, which can be expressed as follows

$$x(t) = \left(A_s + A_r \cos\left(\int_0^T 2\pi\left(\overline{f_r} + \Delta f_r(t)\right)dt + \phi_r\right)\right)\cos(2\pi f_s t + \phi_s) \quad (20)$$

where, $A_s = 2$, $f_s = 50$ and $\phi_s = \pi/6$ are the amplitude, frequency and phase of the supply current signal. $A_r = 0.4$ and $\phi_r = 0$ are the amplitude and phase of the rotating frequency signal. $\overline{f_r} = 24$ is the average of the rotating frequency and $\Delta f_r(t)$ represents the random speed oscillation. Usually, the motor and gear rotor has a relatively large moment of inertia, and the random torque oscillation induced angular speed oscillation is smooth and small. The smooth function was applied after the normally distributed random function to create a smoothly nonstationary variation. The sampling frequency in the simulation study is 5000Hz and the length of the simulated signal is 5 seconds.

Fig. 2 (a) shows the simulated random speed variation in the time domain. Four cases (S1, S2, S3 and S4) are simulated to show the energy leak phenomenon induced by the random speed variation. Among these signals, S1 is the stationary signal without any random speed variation. The other three signals were simulated with increasing speed variation. These four temporal signals displayed in Fig. 2 (b) have obvious modulation characteristics, making it difficult to trace the frequency variation in the time domain.

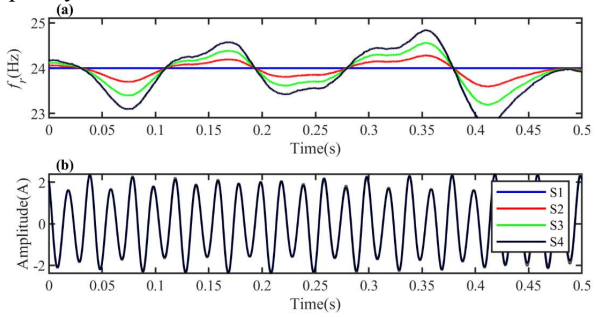

Fig. 2. Simulated signals: (a) random speed oscillation; (b) four temporal signals.

Fig. 3 (a) depicts the time-frequency representation of the lower sideband of the simulated modulation signal S4 by STFT, showing its frequency variation. As shown in Fig. 3 (b), energy leaks into the around bins in the spectrum due to the random speed variation. The theoretical peak value is 0.2, which is shown in the spectrum of signal S1 in Fig. 3 (b). With the increase of the random speed variation, the peak value of the lower sideband decreases gradually from S2 to S4. Therefore, random speed variations significantly influence the accuracy of fault signatures in the dynamic signals of rotating machines.

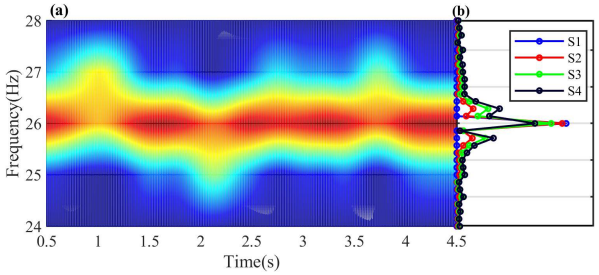

Fig. 3. Spectrum analysis: (a) STFT; (b) spectra.

The simulated signals with different random speed variations were used to compare the performance of the conventional MSB and the proposed Squeezed MSB approaches. White noise was added to the simulated signals to make the Signal to Noise Ratio (SNR) of the noisy signals to be 3dB. Using the simulated signal S4 as an example, Fig. 4 (a) and (c) display the magnitudes of the Squeezed MSB and the conventional MSB, respectively. It is obvious that the modulation component at (24Hz, 50Hz) is very pronounced in the Squeezed MSB result. The surrounding elements are approximately zero, showing effective energy squeezing by the proposed method. In contrast, the conventional MSB has several elements with high magnitudes around the main peak, which denotes the energy leaks in the demodulation process of the nonstationary signals.

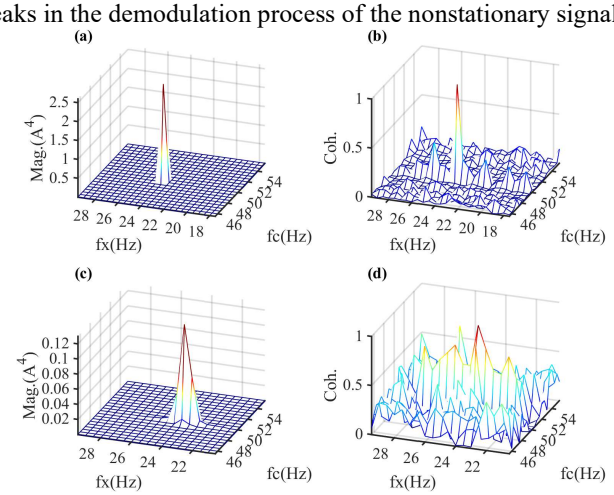

Fig. 4. MSB results of S4: (a) Squeezed MSB magnitude; (b) Squeezed MSB coherence; (c) conventional MSB magnitude; (d) conventional MSB coherence.

The coherence of the Squeezed MSB and the conventional MSB methods of the simulated signal S4 is displayed in Fig. 4 (b) and (d), respectively. As shown in Fig. 4 (b), the sparse coherence of the Squeezed MSB demonstrates the squeezed energy of the coupled components at the bifrequency (24Hz, 50Hz) has high consistency between the bispectrum matrixes. The MSB coherence in Fig. 4 (d) has high values at both the coupled bifrequency and the around bifrequencies. The coherence of the conventional MSB is not sparse because the low magnitude of the main bifrequency cannot highlight the coupled effect of the modulation signal.

Fast-Spectral Correlation (Fast-SC) is a milestone approach for cyclostationary analysis in machine condition monitoring [21]. As explained in the introduction section, the random speed variation cannot be considered as a cyclostationary signal, the Fast-SC of the simulated signal S4 is shown in Fig. 5. Two additional peaks near the rotating frequency are shown in the spectral correlation, which come from the random speed variation in the simulated signals. These additional peaks show that the spectral correlation cannot effectively characterize weak nonstationary signals.

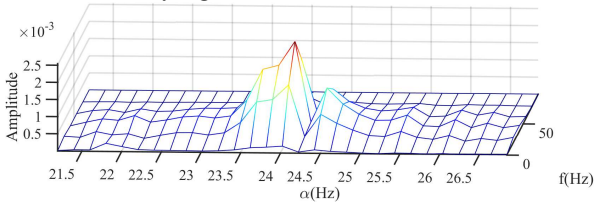

Fig. 5. Fast Spectral Correlation of S4.

The normalized MSB magnitudes and spectral correlation of four simulated signals are shown in Fig. 6 (a). The magnitudes of the conventional MSB decrease by about 20% with the increase of the random speed variation. The Fast-SC performs the worst in these three methods and the amplitude decreases more than 20% with the increase of the nonstationarity. The proposed Squeezed MSB significantly overcome the energy leak effects and maintains the magnitude with less than 5% decrease in the worst simulated scenario. As the coherence of the MSB is not sparse, the maximum value cannot represent the coherent state. Therefore, the Gini index is employed to compare the sparsity of the coherence [22]. The Gini indexes of the MSB coherence are displayed in Fig. 6 (b). The Gini indexes of the Squeezed MSB are more pronounced owing to the better coherence results. The Gini indexes clearly show the proposed method is more reliable when processing nonstationary signals.

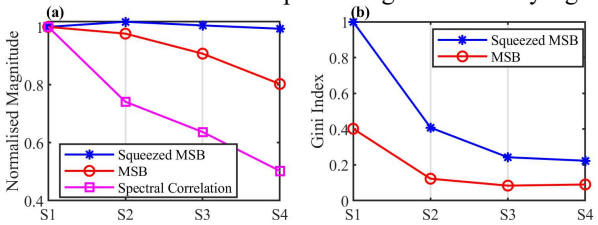

Fig. 6. Results of four simulated signals: (a) normalized magnitude; (b) Gini index of coherence.

IV. Experimental Validation

A. Test Rig and Test Procedure

To evaluate the analysis method in the previous section, an experimental study was conducted on a motor-gear test rig. As shown in Fig. 7 (a), the test rig has a back-to-back configuration of two industrial helical gearboxes which transmit the torque from the induction motor to the DC generator. The components of the rig are connected by flexible couplings for accommodating slight misalignments. The speeds and loads are controlled by a high-performance sensorless variable frequency drive (VFD). Even though, the system exhibits certain speed fluctuation, as shown in Fig. 1, which is mainly due to load fluctuations induced by residual misalignment and manufacture errors. The gearbox 1 (GB1) as the speed reducer has slightly different specifications from the gearbox 2 (GB2) as the speed increaser, which can minimize the influence between the two gearboxes. The gear with the red outline in the GB1 is the target

gear that simulates tooth breakage faults with different severity. The photograph of the test rig is displayed in Fig. 7 (b).

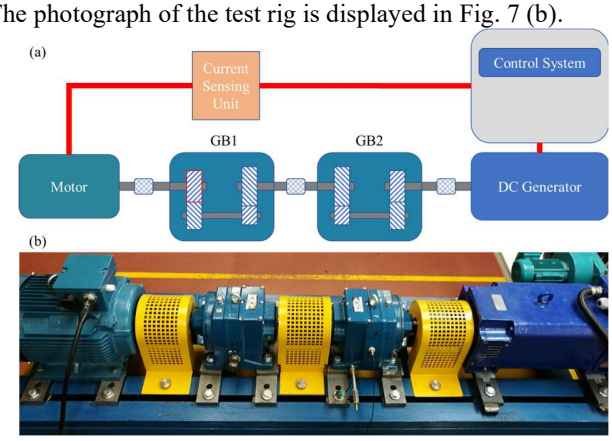

Fig. 7. Test rig: (a) schematic diagram; (b) photography.

The key specifications of the test facilities are listed in TABLE I.

TABLE I
SPECIFICATIONS OF THE TEST FACILITIES

Facilities	Model	Key specifications
DAQ device	YE6232B	16 channels, 24 bits, 96 kHz
Current sensor	EL55P2	50 A, 150 kHz bandwidth
Induction motor	T-DA160LA	15 kW at 1460 rpm
Encoder	RI32-O/100	100ppr, 6000rpm
DC generator	CBH5025	17.5 kW at 2100 rpm
Gearbox 1	M07223.6BR C-1	1st stage teeth No.: 58/47 2nd stage teeth No.: 13/59 Transmission ratio: 3.678/1 Total contact ratio: 4.559

Fig. 8 (a) shows the healthy gear, taken as the Baseline. Fig. 8 (b) and (c) display the seeded tooth breakage faults by removing 50% and 100% of a single tooth, respectively. The studied gear pair has a contact ratio of 1.669 and an overlap ratio of 2.89, leading to a total contact ratio of 4.559. The extremely high contact ratio of the gear pair makes the tooth breakage fault induced meshing stiffness vary with a small amplitude. The fault signatures are therefore very weak, and the fault diagnosis of this gear pair is very challenging. Each test case was operated at 100% of the full motor speed and 0%, 30%, 70%, and 100% of the full motor load. For each test condition, the data acquisition device recorded the data for 5 seconds at a sampling rate of 96 kHz. Such a high sampling rate is mainly to collect accurate pulse signals from the encoder at the motor end for speed estimation.

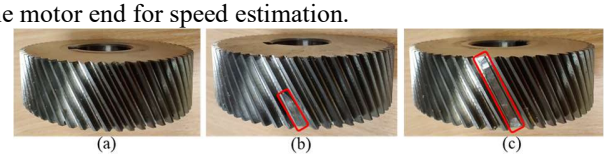

Fig. 8. Seeded gear faults: (a) Baseline; (b) TB50%; (c) TB100%.

B. Comparison of Analysis Results

The spectra of the motor current signals are shown in Fig. 9 (a) and it can be seen that the lower and upper sidebands around the supply frequency are pronounced. The amplitude of the sidebands increases with the loads. To show more details of the sideband, Fig. 9 (b) displays the upper sideband in a narrow frequency band. The sideband under zero load is invisible due to the small torque oscillation. The other three sidebands have high amplitudes in several frequency bins, suggesting that the energy leakage is caused by random speed variations.

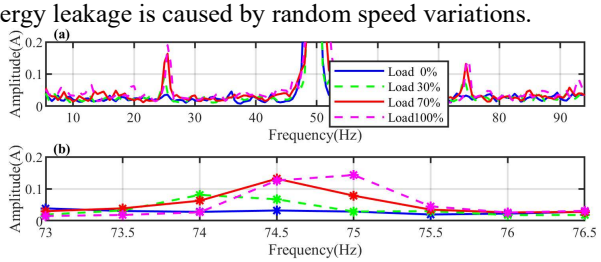

Fig. 9. Spectra of motor current signals: (a) overview; (b) upper sideband.

Both the conventional MSB and the Squeezed MSB results are obtained to compare the accuracy of diagnostics. The conventional MSB magnitudes and coherence at 30% load are shown in Fig. 10 as an example for detailed comparison. The magnitudes of the conventional MSB for Baseline, TB50% and TB100% are depicted in Fig. 10 (a), (c) and (e), respectively. The magnitudes of the modulation frequency (rotating frequency of the gear shaft) are obviously not sparse, especially for the cases of Baseline and TB50%. The coherences in Fig. 10 (b), (d) and (f) show the consistency of the MSB magnitudes at the modulation frequency is very low, which tells the variation between each segment is high and the magnitudes at the modulation frequency are not reliable to diagnose the gear faults. In contrast, the Squeezed MSB method overcomes the random speed variation problem and obtains sparse results of both magnitudes and coherence. As shown in Fig. 11 (a), (c) and (e), the magnitudes at the modulation frequency are sparser than the conventional MSB. The leaked energy is squeezed back to the main lobe and the magnitudes around the modulation frequency are reasonably neglectable. The coherences in Fig. 11 (b), (d) and (f) show that the magnitudes at the modulation frequency are consistent during the ensemble averaging. The high coherence values indicate the extracted fault signatures are reliable for diagnosing the gear faults.

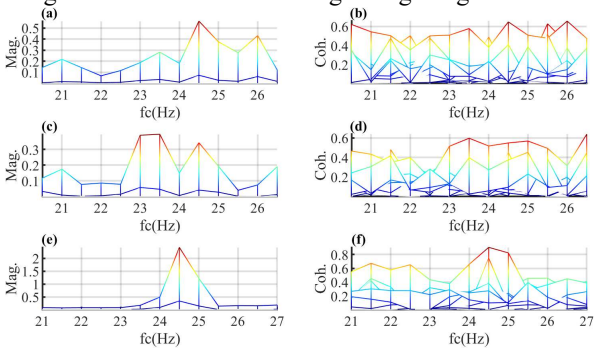

Fig. 10. Convention MSB at 30% load: (a) magnitudes of Baseline; (b) coherence of Baseline; (c) magnitudes of TB50%; (d) coherence of TB50%; (e) magnitudes of TB100%; (f) coherence of TB100%.

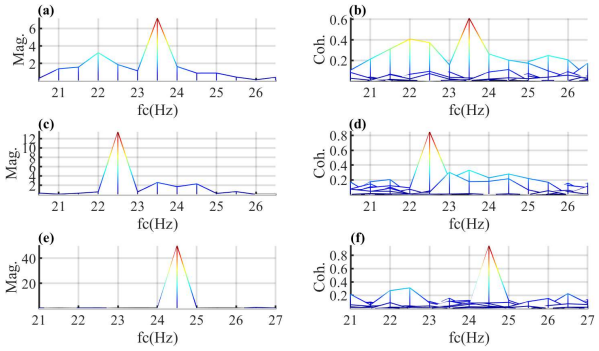

Fig. 11. Squeezed MSB at 30% load: (a) magnitudes of Baseline; (b) coherence of Baseline; (c) magnitudes of TB50%; (d) coherence of TB50%; (e) magnitudes of TB100%; (f) coherence of TB100%.

The magnitudes of the modulation frequency obtained by the Squeezed MSB and the conventional MSB methods are shown in Fig. 12 (a) and (c) respectively. Both approaches give the incremental trend of the magnitudes of the modulation frequency along with the increase of the loads, which is predicted theoretically by (10). However, the challenging issue is to distinguish the fault severity under wide working conditions. Fig. 12 (a) shows that the magnitudes of the Squeezed MSB rise with the increase of the severity of tooth breakage faults under light and heavy loads conditions. The zero load condition is difficult to quantify due to the tiny torque oscillation relating to the gear faults. In general, the Squeezed MSB method can successfully distinguish various fault severity under wide load conditions. In contrast, the conventional MSB method is unable to separate the TB50% faults from the Baseline condition due to the random speed variation.

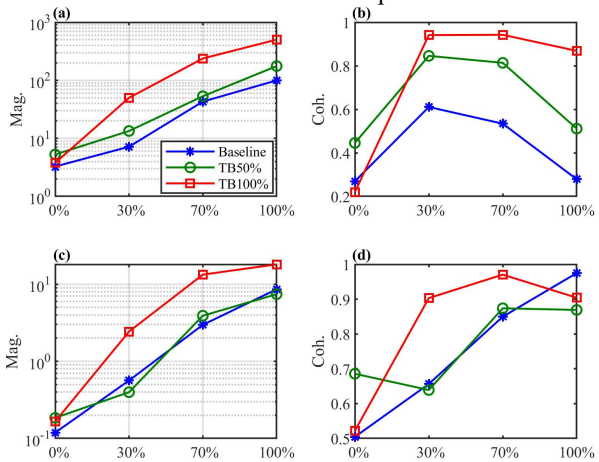

Fig. 12. MSB results of: (a) Squeezed MSB magnitude; (b) Squeezed MSB coherence; (c) conventional MSB magnitude; (d) conventional MSB coherence.

The coherences of the modulation frequency by the Squeezed MSB and the conventional MSB methods are shown in Fig. 12 (b) and (d) respectively. The coherence of the Squeezed MSB shows the consistency of the modulation component increases with the severity of tooth breakage faults. However, the trend of the coherences against the loads is not linear. The coherences of the modulation frequency at medium loads are high, which shows the motor-gear system works at a relatively stable working condition, has less random speed variation and hence generates more consistent fault signatures. The coherences at zero and 100% loads are low because the extreme working conditions make the motor-gear system operate with more uncertainty. The coherences of the conventional MSB method give an increasing trend with the loads at the first glance. However, the coherences are not reliable because the coherences of the non-modulation components are also falsely high. The results of Fast-SC are shown in Fig. 13 and it can be seen that the Fast-SC cannot distinguish the TB50% faults from the Baseline at 30% and 100% loads.

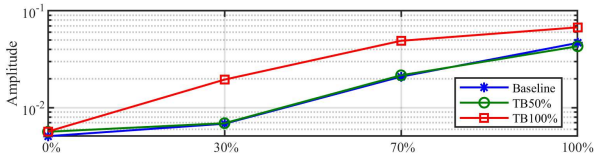

Fig. 13. Fast-SC Results

V. Conclusions

The random speed variation under constant working conditions seems neglectable but actually, it cannot be ignored for accurate fault detection and diagnosis. The random speed variation is not the frequently mentioned phase noise, and the main difference is that the phase noise raises the noise floor other than spreads energy into the around frequency bins. The random speed variation alters the modulation frequency randomly and slowly, which cannot be described by the deterministic frequency modulation. This paper brings the random speed variation into view for the purpose of accurate and reliable fault diagnosis. To restore the attenuated fault signatures, a Squeezed Modulation Signal Bispectrum approach is developed to concentrate the leaked energy back to the main modulation frequency for reliable fault diagnosis of gears. The experimental studies show that the proposed Squeezed MSB method can successfully diagnose gear faults using motor current signals with random speed variations under so-called stationary working conditions. The frequency assignment operator is not robust enough to extremely strong background noise by nature and the proposed Squeezed MSB inevitably inherits the disadvantageous characteristics. Hence, future work should be devoted to increasing the noise robustness and decreasing computational costs.

References

[1] Y. Guo, L. Zhao, X. Wu, and J. Na, 'Tooth root crack detection of planet and sun gears based on resonance demodulation and vibration separation', *IEEE Transactions on Instrumentation and Measurement*, vol. 69, no. 1, pp. 65–75, Jan. 2020, doi: 10.1109/TIM.2019.2893011.

[2] Z. Feng, X. Chen, and M. J. Zuo, 'Induction motor stator current AM-FM model and demodulation analysis for planetary gearbox fault diagnosis', *IEEE Transactions on Industrial Informatics*, vol. 15, no. 4, pp. 2386–2394, Apr. 2019, doi: 10.1109/TII.2018.2875447.

[3] E. Elbouchikhi, V. Choqueuse, F. Auger, and M. E. H. Benbouzid, 'Motor Current Signal Analysis Based on a Matched Subspace Detector', *IEEE Transactions on Instrumentation and Measurement*, vol. 66, no. 12, pp. 3260–3270, Dec. 2017, doi: 10.1109/TIM.2017.2749858.

[4] A. R. Mohanty and C. Kar, 'Fault detection in a multistage gearbox by demodulation of motor current waveform', *IEEE Transactions on*

Industrial Electronics, vol. 53, no. 4, pp. 1285–1297, Jun. 2006, doi: 10.1109/TIE.2006.878303.

[5] J. Zhang, J. S. Dhupia, and C. J. Gajanayake, 'Stator Current Analysis From Electrical Machines Using Resonance Residual Technique to Detect Faults in Planetary Gearboxes', *IEEE Transactions on Industrial Electronics*, vol. 62, no. 9, pp. 5709–5721, Sep. 2015, doi: 10.1109/TIE.2015.2410254.

[6] A. Gao, Z. Feng, and M. Liang, 'Permanent magnet synchronous generator stator current AM-FM model and joint signature analysis for planetary gearbox fault diagnosis', *Mechanical Systems and Signal Processing*, vol. 149, p. 107331, Feb. 2021, doi: 10.1016/j.ymssp.2020.107331.

[7] F. Gu, Y. Shao, N. Hu, A. Naid, and A. D. Ball, 'Electrical motor current signal analysis using a modified bispectrum for fault diagnosis of downstream mechanical equipment', *Mechanical Systems and Signal Processing*, vol. 25, no. 1, pp. 360–372, Jan. 2011, doi: 10.1016/j.ymssp.2010.07.004.

[8] F. Gu, T. Wang, A. Alwodai, X. Tian, Y. Shao, and A. D. Ball, 'A new method of accurate broken rotor bar diagnosis based on modulation signal bispectrum analysis of motor current signals', *Mechanical Systems and Signal Processing*, vol. 50–51, pp. 400–413, Jan. 2015, doi: 10.1016/j.ymssp.2014.05.017.

[9] R. Zhang, F. Gu, H. Mansaf, T. Wang, and A. D. Ball, 'Gear wear monitoring by modulation signal bispectrum based on motor current signal analysis', *Mechanical Systems and Signal Processing*, vol. 94, pp. 202–213, Sep. 2017, doi: 10.1016/j.ymssp.2017.02.037.

[10] R. B. Randall, 'A new method of modeling gear faults', *J. Mech. Des*, vol. 104, no. 2, pp. 259–267, Apr. 1982, doi: 10.1115/1.3256334.

[11] N. Afrizal and R. Ferrero, 'Leakage Error Compensation in Motor Current Signature Analysis for Shaft Misalignment Detection in Submersible Pumps', *IEEE Transactions on Instrumentation and Measurement*, vol. 69, no. 11, pp. 8821–8830, Nov. 2020, doi: 10.1109/TIM.2020.2998301.

[12] Y. Li, H. Zhao, W. Fan, and C. Shen, 'Generalized Autocorrelation Method for Fault Detection Under Varying-Speed Working Conditions', *IEEE Transactions on Instrumentation and Measurement*, vol. 70, pp. 1–11, 2021, doi: 10.1109/TIM.2021.3104018.

[13] J. Antoni, 'Cyclostationarity by examples', *Mechanical Systems and Signal Processing*, vol. 23, no. 4, pp. 987–1036, May 2009, doi: 10.1016/j.ymssp.2008.10.010.

[14] E. Bechhoefer and M. Kingsley, 'A review of time synchronous average algorithms', in *Annual conference of the prognostics and health management society*, San Diego, CA, Sep. 2009, vol. 23, pp. 1–10.

[15] Y. Xu, C. Fu, N. Hu, B. Huang, F. Gu, and A. D. Ball, 'A phase linearisation–based modulation signal bispectrum for analysing cyclostationary bearing signals', *Structural Health Monitoring*, vol. 20, no. 3, pp. 1231–1246, May 2021, doi: 10.1177/1475921720949827.

[16] Y. Xu, G. Feng, X. Tang, S. Yang, F. Gu, and A. D. Ball, 'A Modulation Signal Bispectrum Enhanced Squared Envelope for the detection and diagnosis of compound epicyclic gear faults', *Structural Health Monitoring*, p. 14759217221098576, May 2022, doi: 10.1177/14759217221098577.

[17] T. Oberlin, S. Meignen, and V. Perrier, 'The fourier-based synchrosqueezing transform', in *2014 IEEE International Conference on Acoustics, Speech and Signal Processing (ICASSP)*, May 2014, pp. 315–319. doi: 10.1109/ICASSP.2014.6853609.

[18] S. Wang, X. Chen, C. Tong, and Z. Zhao, 'Matching Synchrosqueezing Wavelet Transform and Application to Aeroengine Vibration Monitoring', *IEEE Transactions on Instrumentation and Measurement*, vol. 66, no. 2, pp. 360–372, Feb. 2017, doi: 10.1109/TIM.2016.2613359.

[19] J. Yuan, Z. Yao, Q. Zhao, Y. Xu, C. Li, and H. Jiang, 'Dual-Core Denoised Synchrosqueezing Wavelet Transform for Gear Fault Detection', *IEEE Transactions on Instrumentation and Measurement*, vol. 70, pp. 1–11, 2021, doi: 10.1109/TIM.2021.3094838.

[20] G. Thakur, E. Brevdo, N. S. Fučkar, and H.-T. Wu, 'The Synchrosqueezing algorithm for time-varying spectral analysis: Robustness properties and new paleoclimate applications', *Signal Processing*, vol. 93, no. 5, pp. 1079–1094, May 2013, doi: 10.1016/j.sigpro.2012.11.029.

[21] J. Antoni, G. Xin, and N. Hamzaoui, 'Fast computation of the spectral correlation', *Mechanical Systems and Signal Processing*, vol. 92, pp. 248–277, Aug. 2017, doi: 10.1016/j.ymssp.2017.01.011.

[22] Y. Miao, J. Wang, B. Zhang, and H. Li, 'Practical framework of Gini index in the application of machinery fault feature extraction', *Mechanical Systems and Signal Processing*, vol. 165, p. 108333, Feb. 2022, doi: 10.1016/j.ymssp.2021.108333.

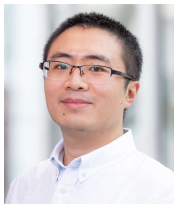

Yuandong Xu received his Ph.D. degree in mechanical engineering from the University of Huddersfield, Huddersfield, UK, in 2020. After graduation, he works as a Research Associate with the Dynamics Group, Department of Mechanical Engineering at Imperial College London. He focuses on vibro-acoustic signal processing for condition monitoring and fault diagnosis of bearings, gears and engines. He has rich experience in vibro-acoustic testing, dynamic modelling, advanced signal processing methods, experimental/operational modal analysis.

Xiaoli Tang received Ph.D. degree in mechatronics engineering from the University of Huddersfield, UK, in 2020. She is currently a KTP associate at Aston University and RL Automotive LTD since August 2021. She worked as a Research Fellow with the School of Engineering and Technology at Aston University, UK, for one and a half years. Her research interests include the development of low-power wireless sensor networks for online condition monitoring of rotating machines, data fusion and compression for machine condition monitoring, machine learning, and energy harvesting.

Xiuquan Sun is currently a Research Fellow at the Centre for Efficiency and Performance Engineering, University of Huddersfield. He received his Ph.D. degree in June 2021. His study focuses on the dynamic behaviors of helical gear induced by tooth wear. He also has tremendous experience in the condition monitoring and fault diagnosis of rotating machinery such as gearboxes, bearings, reciprocating compressors, IC engines, and induction motors.

Fengshou Gu received his Ph.D. degree from the University of Manchester, Manchester, UK, in 2008. He is currently a Professor at the University of Huddersfield, Huddersfield, U.K. He is one of the experts in the fields of machinery diagnosis and vibroacoustic analysis, with over 30 years of research experience. His research interests include system modelling, advanced sensing technologies, advanced signal processing methods, fault diagnosis and condition monitoring.

Andrew D. Ball obtained BEng degree from the University of Leeds and received a Ph.D. from the University of Manchester, UK. He is currently a Professor and Pro-Vice Chancellor at the University of Huddersfield. He is one of the UK's foremost experts in the fields of machinery diagnostics, dynamic modelling, intelligent computation and vibro-acoustics analysis, with over 30 years of maintenance engineering experience in machine diagnosis, non-destructive measurement and related fields, and he spends much of his time lecturing and consulting to the industry in all parts of the world.